University of Dundee

Preclinical Evaluation of AZ12601011 and AZ12799734, Inhibitors of Transforming Growth Factor β Superfamily Type 1 Receptors.

Spender, Lindsay C.; Ferguson, G. John ; Hughes, Gareth D.; Davies, Barry R.; Goldberg, Frederick W.; Herrera, Blanca

Document Version
Peer reviewed version

[Link to publication in Discovery Research Portal](#)

Title: Preclinical evaluation of AZ12601011 and AZ12799734, inhibitors of transforming growth factor beta superfamily type 1 receptors

Authors: Lindsay C. Spender, G. John Ferguson, Gareth D. Hughes, Barry R. Davies, Frederick W. Goldberg, Blanca Herrera, Richard G.Taylor, Lauren S. Strathearn, Owen J. Sansom, Simon T. Barry and Gareth J. Inman

Affiliations: Cancer Research UK Beatson Institute Garscube Estate, Switchback Road, Bearsden, Glasgow G61 1BD, United Kingdom (L.C.S., B.H., G.J.F., O.J.S, G.J.I.) Current addresses: Department of Respiratory, Inflammation and AutoImmunity Research, MedImmune Limited, Cambridge, UK (G.J.F.). Division of Cellular Medicine (R.G.T, L.S.S) and Division of Molecular and Clinical Medicine (L.C.S), School of Medicine, University of Dundee, Dundee, DD1 9SY, United Kingdom. AstraZeneca Bioscience, Oncology, IMED Biotech Unit, AstraZeneca, Cambridge, UK (S.T.B., G.D.H., B.J.D.) Medicinal Chemistry, Oncology, IMED Biotech Unit, AstraZeneca, Cambridge, UK (F.W.G.). Dept. Biochemistry and Molecular Biology, Faculty of Pharmacy, Complutense University of Madrid, Health Research Institute of the Hospital Clínico San Carlos, Madrid, Spain (B.H.)

Running Title: Preclinical evaluation of TGFBR1 inhibitors

Correspondence:

Gareth J. Inman

Cancer Research UK Beatson Institute,

Garscube Estate,

Swithcback Road,

Bearsden,

Glasgow G61 1BD

Tel: (+44) 141 3303654 383366.

EMAIL: g.inman@beatson.gla.ac.uk

Text pages: 29

Tables: 0

Figures: 7

References: 34

Abstract word count: 249

Introduction word count: 778

Discussion word count: 730

Abbreviations: Activin A receptor type 1L (ALK1); Activin A receptor type 1 (ALK2); Activin A Receptor Type 1B (ALK4), Activin A receptor type 1C (ALK7), Bone morphogenetic protein receptor type 1A (BMPR1A); Bone morphogenetic protein receptor type 1B (BMPR1B); GDF2, Growth Differentiation Factor 2 (BMP9); ERK, extracellular signal-regulated kinase; Transforming Growth Factor Beta Receptor 1, (TGFBR1).

MOL#112946

ABSTRACT

The transforming growth factor beta (TGFβ) superfamily includes TGFβ, activins, inhibins and bone morphogenetic proteins (BMPs). These extracellular ligands have essential roles in normal tissue homeostasis by co-ordinately regulating cell proliferation, differentiation, and migration. Aberrant signalling of superfamily members, however, is associated with fibrosis as well as tumourigenesis, cancer progression, metastasis and drug-resistance mechanisms in a variety of cancer sub-types. Given their involvement in human disease, the identification of novel selective inhibitors of TGFβ superfamily receptors is an attractive therapeutic approach. Seven mammalian type 1 receptors have been identified that have context specific roles depending on the ligand and the complex formation with the type 2 receptor. Here we characterise the biological effects of two TGFBR1 kinase inhibitors designed to target TGFβ signalling. AZ12601011 (structure previously undisclosed) and AZ12799734 (IC50s, 18nM and 47nM respectively) were more effective inhibitors of TGFβ-induced reporter activity than SB-431542 (IC50, 84nM) and LY2157299 (galunisertib) (IC50, 380nM). AZ12601011 inhibited phosphorylation of SMAD2 via the type 1 receptors ALK4, TGFBR1 and ALK7. AZ12799734, however, is a pan TGF/BMP inhibitor, inhibiting receptor-mediated phosphorylation of SMAD1 by ALK1, BMPR1A and BMPR1B and phosphorylation of SMAD2 by ALK4, TGFBR1 and ALK7. AZ12601011 was highly effective at inhibiting basal and TGFβ-induced migration of HaCaT keratinocytes and furthermore inhibited tumour growth and metastasis to the lungs in a 4T1 syngeneic orthotopic mammary tumour model. These inhibitors provide new reagents for investigating *in vitro* and *in vivo* pathogenic processes and the contribution of TGFβ and BMP regulated signalling pathways to disease states.

3

INTRODUCTION

The Transforming Growth Factor-β cytokine superfamily, including TGFβ, activin, inhibins, nodal and bone morphogenetic proteins (BMPs), regulate developmental and cellular biology to control and maintain tissue homeostasis. In different contexts, the interaction of the dimeric ligands with their cognate receptors activate intracellular signalling pathways to control cell death, survival, adhesion, differentiation, movement and deposition of components of the extracellular matrix (Shi and Massague, 2003). In human disease the expression of, or cellular responses to, these factors may become deregulated. The resulting aberrant signalling can contribute to many disease pathologies including cancer, fibrosis, atherosclerosis and scarring (Blobe et al., 2000). TGFβ, for example, can switch from tumour suppressor to tumour promoter functions depending on epigenetic/genetic changes occurring in the tumour cell (Inman, 2011). Given their extensive role in human disease, the ligands, their receptors and their downstream effectors are considered attractive therapeutic targets (Akhurst and Hata, 2012).

Cytokine signalling is initiated by the formation of heterotetrameric complexes of six polypeptides comprising dimeric ligands, two constitutively active type 2 receptors and two type 1 receptors. Upon complex formation, the serine/threonine kinase type 1 receptors are phosphorylated and activated by the type 2 receptors which initiates a canonical signalling cascade involving the recruitment, phosphorylation and activation of receptor-regulated SMADs. The phosphorylated SMADs bind to SMAD4 and the complexes accumulate in the cell nucleus where they both positively and negatively regulate gene expression. In addition, a number of SMAD-independent non-canonical signalling pathways (e.g. mitogen-activated protein kinases, Rho GTPases and phosphoinostide-3-kinases) are also activated which impact on gene regulation and cellular responses (Zhang, 2009). Five type 2 and seven type 1 receptors have been identified in mammalian cells. Their specificity for ligand and receptor complex formation determines biological outcome (Schmierer and Hill, 2007). For instance, TGFβ interacts primarily with TGFBR2 and the ubiquitous type 1 receptor TGFBR1 to regulate cytostasis, apoptosis and epithelial to mesenchymal transition (EMT), but both TGFβ and GDF2 (BMP9) may bind to the endothelial cell restricted type 1 receptor ACVRL1 to regulate angiogenesis. In some circumstances, TGFβ may also signal via TGFBR1 and ALK2 to induce SMAD1/5 phosphorylation

and a subset of TGFβ-inducible genes involved in EMT (Ramachandran et al., 2018). BMPs, meanwhile, bind selectively to BMPR2 and the type 1 receptors activin A receptor type 1L (ALK1), activin A receptor type 1 (ALK2), bone morphogenetic protein receptor type 1A (BMPR1A), and bone morphogenetic protein receptor type 1B (BMPR1B) to regulate embryogenesis and bone formation (Wang et al., 2014). TGFβ, Activin and Nodal signal via TGFBR1, ALK4 and ALK7, respectively, predominantly to phosphorylate and activate SMAD2 and SMAD3 while BMPs induce phosphorylation of SMAD1, SMAD5 and SMAD8.

Given the role of TGFβ in pathological states, there have been numerous therapeutic approaches taken to blockade signalling with some progressing through preclinical evaluation to clinical trial (Akhurst and Hata, 2012; Lahn et al., 2005). Some selective small molecule inhibitors (SMI) of the TGFBR1 kinase are well characterised (e.g. SB-431542) (Inman et al., 2002; Vogt et al., 2011) and have been used extensively in preclinical models to interrogate TGFβ-regulated biological pathways. SMIs of TGFBR1 have shown therapeutic promise in models of fibrosis (Gellibert et al., 2006; Park et al., 2015a; Park et al., 2015b), and two TGFBR1 inhibitors are currently in clinical trials, vactosertib (TEW-7197) and galunisertib (LY2157299). The results of the first in human trials with vactosertib (ClinicalTrials.gov Identifier: NCT02160106) are not yet reported. Galunisertib, however, has progressed despite some initial toxicity concerns, and is now considered safe enough when administered with careful dosing schedules (Fujiwara et al., 2015; Herbertz et al., 2015; Kovacs et al., 2015), to allow further clinical development in cancer patients with unmet need. TGFBR1 inhibitors therefore remain attractive leads for drug development.

AZ12601011 (structure previously undisclosed) and AZ12799734 (Anderton et al., 2011; Goldberg et al., 2009) are two selective TGFBR1 inhibitors. AZ12601011 and AZ12799734 inhibit TGFBR1 kinase activity (competition binding) with Kd values of 2.9nM and 740nM, respectively. Both compounds have some inhibitory activity against the related receptors ALK4 and BMPR1B, but are only weakly active against ALK1, ALK2 and BMPR1A in *in vitro* kinase assays (Anderton et al., 2011). Here, we characterise their specificity and *in vitro* and *in vivo* biological activity in a variety of cell-based biochemical and functional assays, in comparison with other well studied and clinically relevant

TGFBR1 SMIs. We show that AZ12601011 is a selective inhibitor of ALK4, ALK7 and TGFBR1. Importantly, AZ12601011 inhibited TGFβ-induced epithelial cell migration at 10-fold lower concentrations than galunisertib and was effective in an *in vivo* tumour model system. Additionally, we identify AZ12799734 as a pan BMP/TGFβ inhibitor providing a novel spectrum of single agent inhibitory activity useful for analytical evaluation of TGFβ superfamily regulated processes.

MATERIALS AND METHODS

Synthetic procedures for AZ12799734 have been described previously (Compound 19, (Goldberg et al., 2009)

Synthetic procedures for AZ12601011:

2-Pyridin-2-yl-1,5,6,7-tetrahydrocyclopenta[e]pyrimidin-4-one2-Amidinopyridine hydrochloride (7.88 g, 50 mmol) and K_2CO_3 (6.91 g, 50 mmol) were added to methyl 2-oxocyclopentanecarboxylate (commercially sourced) (6.21 mL, 50 mmol) in ethanol (100 mL). The mixture was heated to reflux for 5 hours. While the mixture was still hot, it was acidified by the addition of 2 M aq. HCl (20 mL), and water (30 mL). The mixture was allowed to cool to room temperature overnight and was then was partially concentrated *in vacuo*. The resulting precipitate was collected by filtration, washed with water and diethyl ether and dried *in vacuo* to give the desired product. Additional product was obtained by concentrating the filtrate *in vacuo* and purifying the resulting residue by recrystallisation from ethanol/water. The two batches were combined to afford the title compound (3.63 g, 34%). ^{1}H NMR (DMSO-*d[6]*): 2.04 (2H, quintet), 2.71 (2H, t), 2.88 (2H, t), 7.63 (1H, dd), 8.04 (1H, t), 8.30 (1H, d), 8.73 (1H, d), NH missing; *m/z* MH+ 214.
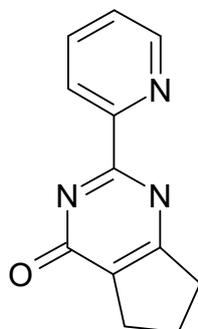

4-Chloro-2-pyridin-2-yl-6,7-dihydro-5*H*-cyclopenta[*d*]pyrimidine POCl$_3$ (4.72 mL, 50.7 mmol) was added to 2-pyridin-2-yl-1,5,6,7-tetrahydro-cyclopenta[*e*]pyrimidin-4-one (2.7 g, 12.7 mmol). The mixture was heated at reflux for 1 hour and was then cooled to room temperature. The mixture was concentrated *in vacuo* and extracted with CH_2Cl_2/CH_3OH. The organic layer was washed sequentially with 5% aq. NaOH and sat. brine, then dried ($MgSO_4$), and concentrated *in vacuo* to afford the title compound (2.60 g, 89%) as a solid. ^{1}H NMR (DMSO-*d[6]*) 2.20 (2H, qn), 3.06 (2H, t), 3.16 (2H, t), 7.79 (1H, t), 8.27 (1H, dt), 8.53 (1H, d), 8.82 (1H, d); *m/z* MH+ 232.
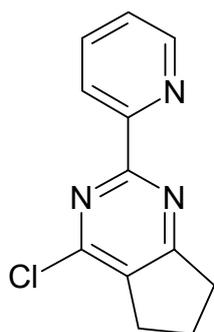
1-(2-Pyridin-2-yl-6,7-dihydro-5*H*-cyclopenta[*e*]pyrimidin-4-yl)pyrrolo[3,2-*c*]pyridine (AZ12601011)

5-Azaindole (1.32 g, 11.1 mmol), Cs_2CO_3 (6.05 g, 18.6 mmol), palladium(II) acetate (0.125 g, 0.56 mmol) and (*R*)-(-)-1-[(*S*)-2-(dicylohexylphosphino)ferrocenyl]ethyldi-*tert*-butylphosphine (0.644 g, 1.11 mmol) were added to 4-chloro-2-(pyridin-2-yl)-6,7-dihydro-5*H*-cyclopenta[*d*]pyrimidine (2.15 g, 9.28 mmol) in 1,4-dioxane (46.4 mL) and the mixture was heated at reflux for 3 hours. The mixture was allowed to cool to room temperature then concentrated *in vacuo* to give a brown gum which was partitioned between CH_2Cl_2/water. The organic layer was isolated and dried ($MgSO_4$) and concentrated *in vacuo*. The resulting crude mixture was purified by flash column chromatography, eluting with 0-5% CH_3OH in CH_2Cl_2, to afford the title compound (1.44 g, 50%) as a solid. ^{1}H NMR (DMSO-*d*[6]) 2.21 (2H, quintet), 3.15 (2H, t), 3.28-3.34 (2H, m), 7.01 (1H, dd), 7.58 (1H, dq), 8.01-8.06 (2H, m), 8.45 (1H, d), 8.46 (1H, dt), 8.65 (1H, dt), 8.84 (1H, dq), 9.00 (1H, d); *m/z* MH[+] 314.
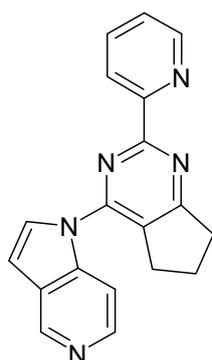
AZ12601011

Plasmids

Plasmids expressing SMAD1 and SMAD2 and constitutively active ALK1, ALK2, BMPR1A, ALK4, TGFBR1, BMPR1B and ALK7 used in transient transfections have been described previously (Inman et al., 2002).

Cell culture

HaCaT, C2C12, T47D, VU-SCC-040, NIH3T3, NIH 3T3-CAGA12-luc, C2C12-BRE-luc and murine 4T1 [4T1-Luc (RRID:CVCL_J239)] cell lines were maintained in DMEM supplemented with 10% FBS and glutamine. Media for NIH 3T3-CAGA12-luc cells was also supplemented with 400mg/mL G418, media for C2C12-BRE-luc was supplemented with 700mg/mL G418. All cells lines were confirmed negative for mycoplasma contamination by the Institute's mycoplasma testing service. Cells were exogenously stimulated with TGFβ1 (Peprotec) resuspended in 1mg/mL BSA/4mM HCl. Inhibitors were diluted in DMSO at 1000-2000x final concentration required. Appropriate BSA/HCl and DMSO vehicle controls were used throughout. Osmotic shock was induced by treatment of cells for 20 minutes with 0.7M NaCl prepared in DMEM and was used to induce p38 MAPK phosphorylation (Davis, 2000). Epidermal growth factor (EGF) treatment was carried out by exogenous addition of 30ng/mL EGF for 5 minutes. The MEK1/2 inhibitor U0126 (Tocris) was used at a concentration of 25μM.

C2C12-BRE luciferase and NIH3T3-CAGA$_{12}$ luciferase reporter bioassays

The C2C12-BRE-luciferase (Herrera and Inman, 2009) and NIH3T3-CAGA12-luciferase stable cell lines (Spender et al., 2016) used in the bioassays have been described previously. Cells were seeded overnight at 1×10^4/well in 96-well plates. Cells were then pre-treated for 20 minutes with a titration of SB-431542 (Inman et al., 2002) (Tocris), SB-525334 (Sigma), AZ12601011 (Anderton et al., 2011), AZ12799734 (AstraZenica) or LY2157299 (galunisertib) (Selleck) followed by stimulation with exogenous TGFβ (1ng/mL) or BMPs. Cell lysates were analysed by the Luciferase Assay system (Promega) as recommended by the manufacturer. The mean percent activity (± S.D) of the reporter in the presence of the inhibitors relative to maximal activation induced by TGFβ or BMPs (100%) is shown.

Dose response IC$_{50}$ (Dm) calculation and proliferation curve analysis

IC$_{50}$ values were determined by curve fitting using either non-linear regression (Graphpad Prism 7) or CalcuSyn Version 2.11 software (Biosoft, UK) which reports median-effect plots, the median dose

(Dm, IC$_{50}$) and the correlation coefficient (r). 95% confidence intervals of IC50 were determined using Graphpad Prism 7 software. Statistical analysis of cell proliferation curves was carried out by pairwise comparison between two or more groups of growth curves using the compareGrowthCurves function from statmod (R project). The number of permutations nsim=10000, p values given were adjusted for multiple testing.

Western blotting and antibodies.

Cell lysates were analysed by SDS-PAGE using the following antibodies: phospho-SMAD2 (Ser465/467) (rabbit polyclonal, #3101, Cell Signalling Technology [CST]), phospho-SMAD1 (rabbit polyclonal, #9511, CST, phospho-ERK (rabbit polyclonal phospho p44/42 (Thr202/Tyr204) MAPK, #9101, CST), phospho-p38 (Thr180/Tyr182) (rabbit polyclonal, #9211, CST), SMAD1 (rabbit polyclonal #38-5400, Zymed), SMAD2 (mouse monoclonal, C16D3, CST), SMAD2/3 (mouse monoclonal, Clone 18, BD transduction Laboratories). Secondary HRP-conjugated antibodies (Dako) and enhanced chemiluminescence (GE Healthcare) was used to detect bound antibody. LI-COR infrared imaging was carried out using a LI-COR Odyssey system following western blotting using rabbit monoclonal anti-phospho-SMAD2 (Ser465/467) (138D4), #3108, CST and mouse monoclonal pan-SMAD2 antibody (L16D3) #3103 CST. Secondary antibodies were IRDye® 680RD Donkey (polyclonal) anti-Rabbit IgG (H+L), #925-68073, LI-COR and IRDye® 800CW goat anti-mouse IgG (H + L), #926-32210, LI-COR. Analysis of signal intensities was carried out using LI-COR Image Studio v4.0.21 software. Signal was normalised to pan-SMAD2 levels measured on channel 800 according to the manufacturer's signal protein normalisation strategy (SPS).

Wound healing assay, IncuCyte Zoom and data analysis

An IncuCyte Zoom live cell imaging microscope (Essen Biosciences) with 10x objective and data management software was used to monitor cell migration in wound healing assays. HaCaT cells were seeded overnight in 100mL growth media at 15000 cells/well in 96-well ImageLock plates (Essen Bioscience). Cells were washed twice in PBS and serum starved for 24 hours in DMEM supplemented

with 0.2% FBS to minimise proliferation which would interfere with migration assays. Uniform wounds were then generated using a Woundmaker, the cells washed twice in PBS, and then pre-treated for 20 minutes with titrations of LY2157299 (galunisertib), SB-431542, AZ12601011 or AZ12799734 in DMEM/0.2% FBS. Cells were then treated with BSA/HCL as a carrier control or TGFβ (5ng/mL). Closure of the wound was monitored by IncuCyte Zoom imaging over 4 days. Data presented is the mean ± S.E.M of a minimum of three replicate wells taken from a representative experiment. The mean ± SEM relative wound density were determined according to software processing definitions as recommended by the manufacturer.

In vivo 4T1 syngeneic orthotopic mammary fat-pad model for efficacy and PK/PD

The 4T1 cell line was maintained in RPMI 1640 (Invitrogen) supplemented with 10% FCS (Sigma Aldrich) and M1 (Egg Technologies) with 1% glutamine (Invitrogen) in 7.5% CO_2 at 37°C and were detached using 0.05% trypsin (Invitrogen). Cells were implanted in to mammary fat pad 4 in 30μL PBS/A at $1x10^4$ per mouse. Female BALB/c mice (Charles River) at greater than 18g had tumour sizes monitored three times weekly by bilateral caliper measurements. Tumour volume was calculated at each measure with dosing from the day following implant. Controls received vehicle only (0.5% Methocel E4 Premium / 0.1% Polysorbate 80) by oral gavage twice daily for the duration of the study. The treatment group received AZ12601011 50mg/kg twice daily in 0.5% Methocel / 0.1% Polysorbate. Samples for PK and PD analysis were sampled at 1 and 6h post final AM dose on Day 25. Additionally, lung samples were taken to assess the number of lung metastases. Following formalin fixation each lobe was sectioned, creating five serial sections per lobe, 200μm apart. The sections were then stained with haematoxylin and eosin stain and the number of metastases counted using light microscopy. This study was run in the UK in accordance with UK Home Office legislation, the Animal Scientific Procedures Act 1986 (ASPA) and with AstraZeneca Global Bioethics policy. Experimental details are outlined in Home Office Project Licence 40/2934. Additional dosing was undertaken for PK profile analysis for AZ12601011 and AZ12799734 at 50mg/kg per oral dose in male nude mice in vehicle as detailed above. Statistical analysis was carried out using SPSS software (IBM).

MOL#112946

In vivo pharmacokinetic analysis

Each plasma sample (25 µl) was prepared using an appropriate dilution factor and compared against

an 11 point standard calibration curve (1-10000 nM) prepared in DMSO and spiked into blank plasma.

Acetonitrile (100 µl) was added with the internal standard, followed by centrifugation at 3000 rpm for

10 minutes. Supernatant (50 µl) was then diluted in 300 µl water and analyzed via UPLC-MS/MS. The

Mass Spectrometer and UPLC parameters are detailed below along with the optimisation parameters.

Mass Specrometer and UPLC system parameters

Mass Spec	Waters Ultima Pt			
HPLC system	Agilent 1100 HPLC			
Column	Waters x-bridge C18 50 x 2.1, 3.5u			
Solvent A	95% Water, 5% MeOH + 10mM Ammonium Acetate			
Solvent B	95% MeOH, 5% Water + 10mM Ammonium Acetate			
Gradient	Time (min)	% A	%B	
	0	95	5	
	3	5	95	
	3.8	5	95	
	3.81	95	5	
	4	95	5	
Flow	0.75 ml/min			
Run time	4 min, use a divert valve for initial 0.5 minutes			

Optimization parameters for mass spectrometry analysis

Compound	Ionization mode	Polarity	Parent ion	Daughter ion	Cone voltage (v)	Collison Energy
AZ12601011	ESI	Positive	314.2076	78.0667	80	46
AZ12799734	ESI	Positive	371.15	290.21	50	34
AZ10024306 (ISTD)	ESI	Positive	408.253	174.189	80	22

In vivo pharmacodynamic analysis of phospho-SMAD2 using ELISA

Mouse total SMAD 2/3 mAB (BD Biosciences Cat 610843l) at 1.25µg/ml in PBS/A was used to coat Greiner black high-bind 96-well plates with incubation for 1hour at room temperature then inverted and blotted. Blocking buffer with 3% BSA (Sigma A-3912) was added and the incubation/blotting process repeated. 4T1 tumour lysate was prepared at 100µg/well in AP lysis buffer containing fresh protease/ phosphatase inhibitors and then added to the wells for an overnight incubation at 4°C. Following this incubation all wells were washed with TBS/T. A plate was incubated with primary antibody (Rabbit Upstate phospho-SMAD2, #05-953) and a second plate was incubated with primary antibody, Rabbit CST Total SMAD 2/3 (CST 3102). Blocking buffer was used for the antibodies and the plates were incubated for 2hours at RT followed by washing with TBS/T. Anti-rabbit HRP conjugate (CST 7074) was added to the plates and incubated for 1hour followed by a further wash. They were developed with Quantablu using the manufacturer's recommended protocol and read on a Tecan SpectroFluor using excitation 340nm / 465nm emission.

RESULTS

AZ12601011 and AZ12799734 inhibit ligand activated SMAD3/4 transcription.

NIH 3T3 cells stably expressing a TGFβ inducible CAGA$_{12}$-luciferase reporter construct were used to

determine the effect of AZ12601011 and AZ12799734 (compound structures are shown in Fig.1A) on

TGFβ-induced transcription in comparison with the previously characterised TGFBR1 inhibitors SB-

431542, SB-525334 and LY2157299 (galunisertib). The 12 tandem copies of the SMAD binding

element CAGA (Dennler et al., 1998) regulate luciferase reporter gene activity in response to TGFβ

receptor regulated SMAD3 and SMAD4 binding. Luciferase activity in cell lysates increased in

response to TGFβ1 addition and was inhibited by all compounds tested (Fig 1B). The IC$_{50s}$, determined

by curve fitting from dose response curves (Fig. 1C) of AZ12601011 (18 ± 6nM) and AZ12799734 (47

± 7nM), were lower than those of the other inhibitors and were approximately 10-fold lower than the

IC$_{50}$ of galunisertib (384 ± 170nM) approved for use in clinical trials (Figs 1C and 1D). Phosphorylation

of SMAD2 induced by exogenous TGFβ addition, detected using a polyconal rabbit anti-

phosphorylated SMAD2 (ser465/467) antibody, was completely inhibited by the most active inhibitor

AZ12601011 in four cell lines at concentrations between 300nM and 1μM (Fig. 2A). The inhibition of

SMAD2 phosphorylation in TGFβ treated HaCaT relative to pan-SMAD2 levels was quantified by LI-

COR infrared imaging using a second monoclonal rabbit anti-phosphorylated SMAD2 (ser465/467)

(138D4) antibody (Fig. 2B-2D). Representative blots are shown in Fig. 2B, and combined raw intensity

traces from channel 700 and 800 scans of lane 2 (control + TGFβ) measuring phospho-SMAD2 and

pan-SMAD2, respectively are shown in Fig. 2C. Normalised phospho-SMAD2 levels relative to un-

induced levels (lane1) are shown in Fig. 2D, these returned to baseline in the presence of 0.3μM

AZ12601011 and indicate similar levels of inhibition as those seen in Fig 2A.

Stability and specificity of AZ12601011 and AZ12799734

We next tested the suitability, stability and specificity of AZ12601011 and AZ12799734 as reagents for

studying TGFβ family signalling in cell based assays. Neither AZ12601011 nor AZ12799734 showed

any reduction in their ability to block CAGA$_{12}$-luciferase reporter activity following up to six rounds of

freeze-thawing when used at concentrations selected to inhibit CAGA12 activity by approximately 50%
(20nM and 60nM, respectively) (Fig. 3A). All four inhibitors tested maintained activity when incubated
in tissue culture medium for up to 10 days (Fig. 3B) and effectively maintained efficacy in *in vitro* cell
culture assays over this time period as assessed by the ability to block TGFβ-mediated induction of
SMAD2 phosphorylation (Fig. 3C). AZ12601011 and AZ12799734 can therefore be used to effectively
block TGFβ signalling in phenotypic assays over a 10 day time course.

Previous drugs designed to target the TGFβ type 1 receptor, such as SB-431542, effectively inhibit the
activity of activin and nodal receptors ALK4 and ALK7 in addition to TGFBR1. Using transient
transfection assays, we therefore also assessed the effect of AZ12601011 and AZ12799734 on
constitutively active ALK4, ALK7 and TGFBR1 receptors expressed in NIH3T3 CAGA$_{12}$ reporter
cells. Induction of CAGA$_{12}$-luciferase reporter activity induced by transient transfection of the
constitutively active receptors is shown in Fig. 4A. Following transient transfection, cells were treated
with a titration of AZ12601011 and AZ12799734 and the effect on CAGA$_{12}$ reporter activity monitored
(Fig. 4B). AZ12601011 inhibited the activity of ALK4, ALK7 and TGFBR1 at concentrations between
0.01μM – 10μM equally. AZ12799734 also inhibited the three constitutively active receptors equally
at concentrations ranging from 1μM – 10μM. We next tested the effect of AZ12601011 and
AZ12799734 on receptor regulated SMAD phosphorylation by transient transfection of constitutively
active receptors into NIH3T3 cells (Fig. 4C). Phosphorylation of co-transfected SMAD1 and SMAD2
by the active receptors was monitored by western blot. All seven receptors induced phosphorylation of
either SMAD1 or SMAD2; as expected, phosphorylation of SMAD1 occurred following transfection
of ALK1, BMPR1A and BMPR1B, and phosphorylation of SMAD2 occurred following transfection of
ALK4, TGFBR1 and ALK7 (Fig. 4C). AZ12601011 inhibited phosphorylation of SMAD2 but not
SMAD1, suggesting that (like SB-431542) AZ12601011 is a selective inhibitor of ALK4, TGFBR1 and
ALK7.

AZ12799734, however, inhibited phosphorylation of both SMAD1 and SMAD2 and is thus likely to be
a pan BMP/TGF receptor inhibitor. The effect of AZ12999734 on BMP signalling was confirmed using
a bioassay measuring the transcriptional activation of a BMP responsive element luciferase reporter

construct (C2C12-BRE-LUC) (Herrera and Inman, 2009) after exogenous addition of BMP4, BMP6 or GDF2 (BMP9). As expected, given that there was no effect of AZ12601011 on SMAD1 phosphorylation, we saw no inhibition of BMP-induced activity of C2C12-BRE-LUC in AZ12601011 treated cells (Fig. 5A). Following treatment by AZ12601011, we observed no inhibition of extracellular signals regulating phosphorylation of ERK (induced by EGF) (Fig5B) or p38 MAPK family members (induced by osmotic shock) (Fig. 5C). AZ12601011 therefore had no inhibitory off-target effect on the EGF-activated EGFR/MEK/ERK signalling cascade (Bogdan and Klambt, 2001) which was efficiently blocked by the MEK1/2 inhibitor, U0126, which was used as a positive control for MEK1/2 inhibition (Fig. 5B).

AZ12601011 and AZ12999734 inhibit TGFβ-induced migration.

AZ12601011 and AZ12799734 were assessed in functional wound healing assays using HaCaT epithelial cells that measure a TGFβ-inducible SMAD4-dependent migration responses (Levy and Hill, 2005). Confluent monolayers of serum-starved (0.2% FBS) HaCaT cells were uniformly scratched using a Woundmaker (Essen Biosciences), and the resulting wound closure was analysed by real time imaging (Fig. 6). Serum starved DMSO control treated cells migrated to close the wound by just over 80% after 80 hours incubation. Following treatment with TGFβ, however, HaCaT cells migrated faster to close the wound entirely within 36 hours. When cells were pre-treated with different concentrations of SB-431542, galunisertib, AZ12601011 or AZ12799734 prior to TGFβ addition, we observed dose-dependent decreases in TGFβ-induced migration. SB-431542, galunisertib, AZ12601011 and AZ12799734 blocked the increase in migration at concentrations of 500nM, 5000nM, 100nM and 500nM, respectively. At 500nM, AZ12601011 reduced cell migration below baseline, which was only achieved at doses ≥5μM of SB-431542 and AZ12799734 (data not shown). AZ12601011 therefore was the most effective inhibitor in the wound healing assay, which inhibited TGFβ-induced migration at concentrations at least 10-fold lower than galunisertib.

AZ12601011 inhibits tumour growth and metastasis *in vivo*.

The selectivity profile of AZ12601011 for ALK4, ALK5 and ALK7 (similar in scope to galunisertib in clinical trials) made it a good representative probe molecule to understand the profile of a TGFBR1 inhibitor *in* vivo, We tested the pharmacokinetics of both drugs (total and free) in BALB/c mice following administration of 50mg/kg dose (Fig. 7A), and tested the effect of AZ12601011 on 4T1 cell proliferation *in vitro* prior to its use in an *in vivo* assay of preventative treatment of 4T1 syngeneic orthotopic tumour growth. AZ12601011 inhibited 4T1 proliferation with an IC_{50} of 400nM (Figure 7B). In the orthotopic *in vivo* assay, AZ12601011 inhibited signalling measured by a reduction in detection of phosphorylated SMAD2 in tumour cell lysates 1 hour after administration (50mg/kg) (Fig.7C). AZ12601011 inhibited 4T1 cells growth in vitro (IC50 = 0.4μM) (Fig.7C). To assess efficacy in vivo, mice were treated twice daily with vehicle or AZ12601011 (50mg/kg) starting the day after implant of 4T1 cells into mammary fat pads. Tumour growth was monitored over 25 days (Fig. 7D). The average tumour size in the treated (n=10) group up to day 18 (when 13/13 mice in the control group remained in the study) was significantly inhibited by AZ12601011 (p=0.0001) compared to controls (n=13) (Fig. 7E). 2/13 mice in the control group had to be sacrificed before the end of the study at days 18 and 23 due to large tumour sizes. No tumours in the treated group exceeded the stipulated size limit and 1/10 mice did not develop a measurable tumour. We noted a significant increase in event-free survival (p=0.002) and in the time taken to develop tumours exceeding $0.5cm^3$ (p<0.005) in the treated mice (Fig. 7F). Importantly, we also found a statistically significant reduction (p = 0.025) in the median lung metastasis score in mice treated with AZ12601011 (median = 1) compared to the control group (median = 4), U = 26, z = -2.267, using an exact sampling distribution for U.

AZ12601011 therefore shows efficacy as a single agent therapy in tumour model systems providing a TGFBR1 inhibitor lead compound for future development.

DISCUSSION

Our data describe the specificity and efficacy of two compounds designed to inhibit TGFBR1 kinase activity (AZ12601011 and AZ12799734) in a number of cell-based assays. We provide evidence that AZ12601011 targets ALK4 and ALK7 as well as TGFBR1, while AZ12799734 is a pan inhibitor of ALK1, ALK2, BMPR1A, ALK4, TGFBR1, BMPR1B and ALK7. Thus, although not directly tested here, we predict that like SB-431542, AZ12601011 will also inhibit activin and nodal signalling through ALK4 and ALK7. AZ127994734, we anticipate, may be useful as a single agent combined inhibitor of TGFβ and BMP activity.

The efficacy of AZ12601011 and AZ12799734 was also assessed in biological assays of TGFβ-induced transcription and migration. TGFβ-induced migration of HaCaT epithelial cells is, in part, reported to involve TGFβ-mediated activation of a genetic program regulated by the ERK signalling pathway demonstrated by the observation that the MEK/ERK inhibitor U2016 can inhibit this response (Zavadil et al., 2001). Since 100nM concentrations of AZ12601011 inhibited migration but had no effect on EGF-induced phosphorylation of ERK or p38 phosphorylation up to concentrations of 10μM, we conclude that the effects of the inhibitors on migration are not a result of off target inhibition of MEK/ERK but are likely a result of on-target TGFBR1 inhibition. In these assays, AZ12601011 and AZ12799734 were at least 10-fold more effective in blocking TGFβ-induced transcription and migration than galunisertib currently in clinical trials. Importantly, AZ12601011 reduced signalling via SMAD2 *in vivo* and also inhibited tumour growth and metastasis of in an orthotopic murine model of breast cancer, suggesting therapeutic potential.

The development of novel inhibitors of TGFBR1 could provide new therapeutic options in TGFβ-associated pathologies such as cancer and fibrosis. The clinical use of TGFBR1 inhibitors, however, is not without concerns over patient safety. TGFβ signalling via TGFBR1 has a role in cardiac development (Sridurongrit et al., 2008) and several heart defects are evident in TGFβ2 null mice. Because increased TGFβ expression is involved in cardiac remodelling in response to numerous stresses (Lim and Zhu, 2006), TGFBR1 inhibitors are predicted to be of benefit in combating the effects of

18

cardiac remodelling in heart failure. However, administration of AZ12601011 to disease-free wild type mice is associated with cardiac toxicity involving the development of aortic lesions (Anderton et al., 2011). Questions over these homeostatic functions of TGFβ have thus delayed development of lead compounds like LY2157299 (galunisertib). Similar effects of galunisertib on small mammals were noted during detailed pre-clinical toxicity testing, but, were ameliorated by lower doses and careful dosing schedules (Herbertz et al., 2015). These concerns therefore appear to be largely overcome and several cancer related trials of galunisertib as a monotherapy, or in combination with other chemotherapeutics, are ongoing. The efficacy of galunisertib in models of cancer, however, appears limited by tumour environmental factors and anti-tumour growth inhibitory effects are lacking in some xenograft models (Herbertz et al., 2015; Maier et al., 2015). In hepatocellular cancer cells, galunisertib had minimal effects on proliferation, but inhibited invasion (Serova et al., 2015). Most of the studies to date have focussed on anti-proliferative and tumour-killing potential in standard assays, and there is growing evidence that these inhibitors may be more effective in cancer models measuring metastasis, immune function and cancer stem cell-like properties (Anido et al., 2010; Maurantonio et al., 2011; Penuelas et al., 2009; Spender et al., 2016). For example, galunisertib has been shown to inhibit TGFβ induced migration and immune suppression *in vitro* (Yingling et al., 2018). In addition, SB-431542 inhibits mutant BRAF melanoma cell migration and stem-cell like properties of anchorage independent growth and clonogenicity at low-cell density. These effects are overcome by increasing cell density leading to the conclusion that the dependence of tumour cells on TGFβ/TGFBR1 signalling is revealed under conditions of cellular stress. TGFBR1 inhibitors may therefore be most effective in inhibiting micrometastasis seeding or outgrowth, following removal of any clinically apparent tumour mass (Spender et al., 2016). This conclusion is supported by the inhibitory effect of AZ12601011 on HaCaT cell migration and the formation of 4T1 lung metastasis in our experimental cell based assays. Hence, TGFβ receptor inhibitors remain candidate therapeutic agents with therapeutic potential, despite the lack of significant tumour killing by galunisertib. Additionally, galunisertib has shown promise in *ex vivo* models of fibrotic disease (Luangmonkong et al., 2017). AZ12601011 and AZ12799734 therefore

provide new tools for studying TGFβ and BMP regulated biological processes and lead compounds for

clinical development.

AUTHORSHIP CONTRIBUTIONS

Participated in research design: Spender, Sansom, Hughes, Goldberg, Davies, Barry, Herrera, Ferguson and Inman.

Conducted experiments: Spender, Ferguson, Taylor, Strathearn, Herrera, Barry, Hughes, Goldberg, Davies and Inman.

Performed data analysis: Spender, Herrera, Ferguson, Taylor, Hughes, Davies, Barry and Inman.

Wrote or contributed to the writing of the manuscript: Spender, Barry, Taylor, Herrera, Sansom, Goldberg, Davies, Hughes and Inman.

Davies, Hughes, Goldberg and Barry are employees and shareholders of AstraZeneca. Ferguson is an employee of an AstraZeneca owned company and is a shareholder of AstraZeneca.

REFERENCES

Akhurst, R.J., and Hata, A. (2012). Targeting the TGFbeta signalling pathway in disease. Nat Rev Drug Discov *11*, 790-811.

Anderton, M.J., Mellor, H.R., Bell, A., Sadler, C., Pass, M., Powell, S., Steele, S.J., Roberts, R.R., and Heier, A. (2011). Induction of heart valve lesions by small-molecule ALK5 inhibitors. Toxicol Pathol *39*, 916-924.

Anido, J., Saez-Borderias, A., Gonzalez-Junca, A., Rodon, L., Folch, G., Carmona, M.A., Prieto-Sanchez, R.M., Barba, I., Martinez-Saez, E., Prudkin, L., *et al.* (2010). TGF-beta Receptor Inhibitors Target the CD44(high)/Id1(high) Glioma-Initiating Cell Population in Human Glioblastoma. Cancer Cell *18*, 655-668.

Blobe, G.C., Schiemann, W.P., and Lodish, H.F. (2000). Role of transforming growth factor beta in human disease. N Engl J Med *342*, 1350-1358.

Bogdan, S., and Klambt, C. (2001). Epidermal growth factor receptor signaling. Curr Biol *11*, R292-295.
Davis, R.J. (2000). Signal transduction by the JNK group of MAP kinases. Cell *103*, 239-252.

Dennler, S., Itoh, S., Vivien, D., ten Dijke, P., Huet, S., and Gauthier, J.M. (1998). Direct binding of Smad3 and Smad4 to critical TGF beta-inducible elements in the promoter of human plasminogen activator inhibitor-type 1 gene. Embo J *17*, 3091-3100.

Fujiwara, Y., Nokihara, H., Yamada, Y., Yamamoto, N., Sunami, K., Utsumi, H., Asou, H., Takahash, I.O., Ogasawara, K., Gueorguieva, I., *et al.* (2015). Phase 1 study of galunisertib, a TGF-beta receptor I kinase inhibitor, in Japanese patients with advanced solid tumors. Cancer Chemother Pharmacol *76*, 1143-1152.

Gellibert, F., de Gouville, A.C., Woolven, J., Mathews, N., Nguyen, V.L., Bertho-Ruault, C., Patikis, A., Grygielko, E.T., Laping, N.J., and Huet, S. (2006). Discovery of 4-{4-[3-(pyridin-2-yl)-1H-pyrazol-4-yl]pyridin-2-yl}-N-(tetrahydro-2H- pyran-4-yl)benzamide (GW788388): a potent, selective, and orally active transforming growth factor-beta type I receptor inhibitor. J Med Chem *49*, 2210-2221.

Goldberg, F.W., Ward, R.A., Powell, S.J., Debreczeni, J.E., Norman, R.A., Roberts, N.J., Dishington, A.P., Gingell, H.J., Wickson, K.F., and Roberts, A.L. (2009). Rapid generation of a high quality lead for transforming growth factor-beta (TGF-beta) type I receptor (ALK5). J Med Chem *52*, 7901-7905.

Herbertz, S., Sawyer, J.S., Stauber, A.J., Gueorguieva, I., Driscoll, K.E., Estrem, S.T., Cleverly, A.L., Desaiah, D., Guba, S.C., Benhadji, K.A., *et al.* (2015). Clinical development of galunisertib (LY2157299 monohydrate), a small molecule inhibitor of transforming growth factor-beta signaling pathway. Drug Des Devel Ther *9*, 4479-4499.

Herrera, B., and Inman, G.J. (2009). A rapid and sensitive bioassay for the simultaneous measurement of multiple bone morphogenetic proteins. Identification and quantification of BMP4, BMP6 and BMP9 in bovine and human serum. BMC Cell Biol *10*, 20.

Inman, G.J. (2011). Switching TGFbeta from a tumor suppressor to a tumor promoter. Current opinion in genetics & development *21*, 93-99.

Inman, G.J., Nicolas, F.J., Callahan, J.F., Harling, J.D., Gaster, L.M., Reith, A.D., Laping, N.J., and Hill, C.S. (2002). SB-431542 is a potent and specific inhibitor of transforming growth factor-beta superfamily type I activin receptor-like kinase (ALK) receptors ALK4, ALK5, and ALK7. Molecular pharmacology *62*, 65-74.

Kovacs, R.J., Maldonado, G., Azaro, A., Fernandez, M.S., Romero, F.L., Sepulveda-Sanchez, J.M., Corretti, M., Carducci, M., Dolan, M., Gueorguieva, I.*, et al.* (2015). Cardiac Safety of TGF-beta Receptor I Kinase Inhibitor LY2157299 Monohydrate in Cancer Patients in a First-in-Human Dose Study. Cardiovasc Toxicol *15*, 309-323.

Lahn, M., Kloeker, S., and Berry, B.S. (2005). TGF-beta inhibitors for the treatment of cancer. Expert Opin Investig Drugs *14*, 629-643.

Levy, L., and Hill, C.S. (2005). Smad4 dependency defines two classes of transforming growth factor {beta} (TGF-{beta}) target genes and distinguishes TGF-{beta}-induced epithelial-mesenchymal transition from its antiproliferative and migratory responses. Mol Cell Biol *25*, 8108-8125.

Lim, H., and Zhu, Y.Z. (2006). Role of transforming growth factor-beta in the progression of heart failure. Cell Mol Life Sci *63*, 2584-2596.

Luangmonkong, T., Suriguga, S., Bigaeva, E., Boersema, M., Oosterhuis, D., de Jong, K.P., Schuppan, D., Mutsaers, H.A.M., and Olinga, P. (2017). Evaluating the antifibrotic potency of galunisertib in a human ex vivo model of liver fibrosis. British journal of pharmacology *174*, 3107-3117.

Maier, A., Peille, A.L., Vuaroqueaux, V., and Lahn, M. (2015). Anti-tumor activity of the TGF-beta receptor kinase inhibitor galunisertib (LY2157299 monohydrate) in patient-derived tumor xenografts. Cell Oncol (Dordr) *38*, 131-144.

Maurantonio, M., Ballestri, S., Odoardi, M.R., Lonardo, A., and Loria, P. (2011). Treatment of atherogenic liver based on the pathogenesis of nonalcoholic fatty liver disease: a novel approach to reduce cardiovascular risk? Archives of medical research *42*, 337-353.

Park, J.H., Ryu, S.H., Choi, E.K., Ahn, S.D., Park, E., Choi, K.C., and Lee, S.W. (2015a). SKI2162, an inhibitor of the TGF-beta type I receptor (ALK5), inhibits radiation-induced fibrosis in mice. Oncotarget *6*, 4171-4179.

Park, S.A., Kim, M.J., Park, S.Y., Kim, J.S., Lee, S.J., Woo, H.A., Kim, D.K., Nam, J.S., and Sheen, Y.Y. (2015b). EW-7197 inhibits hepatic, renal, and pulmonary fibrosis by blocking TGF-beta/Smad and ROS signaling. Cell Mol Life Sci *72*, 2023-2039.

Penuelas, S., Anido, J., Prieto-Sanchez, R.M., Folch, G., Barba, I., Cuartas, I., Garcia-Dorado, D., Poca, M.A., Sahuquillo, J., Baselga, J.*, et al.* (2009). TGF-beta increases glioma-initiating cell self-renewal through the induction of LIF in human glioblastoma. Cancer Cell *15*, 315-327.

Ramachandran, A., Vizan, P., Das, D., Chakravarty, P., Vogt, J., Rogers, K.W., Muller, P., Hinck, A.P., Sapkota, G.P., and Hill, C.S. (2018). TGF-beta uses a novel mode of receptor activation to phosphorylate SMAD1/5 and induce epithelial-to-mesenchymal transition. eLife *7*.

Schmierer, B., and Hill, C.S. (2007). TGFbeta-SMAD signal transduction: molecular specificity and functional flexibility. Nat Rev Mol Cell Biol *8*, 970-982.

Serova, M., Tijeras-Raballand, A., Dos Santos, C., Albuquerque, M., Paradis, V., Neuzillet, C., Benhadji, K.A., Raymond, E., Faivre, S., and de Gramont, A. (2015). Effects of TGF-beta signalling inhibition with galunisertib (LY2157299) in hepatocellular carcinoma models and in ex vivo whole tumor tissue samples from patients. Oncotarget *6*, 21614-21627.

Shi, Y., and Massague, J. (2003). Mechanisms of TGF-beta signaling from cell membrane to the nucleus. Cell *113*, 685-700.

Spender, L.C., Ferguson, G.J., Liu, S., Cui, C., Girotti, M.R., Sibbet, G., Higgs, E.B., Shuttleworth, M.K., Hamilton, T., Lorigan, P.*, et al.* (2016). Mutational activation of BRAF confers sensitivity to transforming growth factor beta inhibitors in human cancer cells. Oncotarget *7*, 81995-82012.

Sridurongrit, S., Larsson, J., Schwartz, R., Ruiz-Lozano, P., and Kaartinen, V. (2008). Signaling via the Tgf-beta type I receptor Alk5 in heart development. Dev Biol *322*, 208-218.

Vogt, J., Traynor, R., and Sapkota, G.P. (2011). The specificities of small molecule inhibitors of the TGFss and BMP pathways. Cell Signal *23*, 1831-1842.

Wang, R.N., Green, J., Wang, Z., Deng, Y., Qiao, M., Peabody, M., Zhang, Q., Ye, J., Yan, Z., Denduluri, S.*, et al.* (2014). Bone Morphogenetic Protein (BMP) signaling in development and human diseases. Genes Dis *1*, 87-105.

Yingling, J.M., McMillen, W.T., Yan, L., Huang, H., Sawyer, J.S., Graff, J., Clawson, D.K., Britt, K.S., Anderson, B.D., Beight, D.W.*, et al.* (2018). Preclinical assessment of galunisertib (LY2157299 monohydrate), a first-in-class transforming growth factor-beta receptor type I inhibitor. Oncotarget *9*, 6659-6677.

Zavadil, J., Bitzer, M., Liang, D., Yang, Y.C., Massimi, A., Kneitz, S., Piek, E., and Bottinger, E.P. (2001). Genetic programs of epithelial cell plasticity directed by transforming growth factor-beta. Proc Natl Acad Sci U S A *98*, 6686-6691.

Zhang, Y.E. (2009). Non-Smad pathways in TGF-beta signaling. Cell Res *19*, 128-139.

MOL#112946

FOOTNOTES

FIGURE LEGENDS

Figure 1. Activity of five TGFBR1 inhibitors in TGFβ-induced SMAD3/4 dependent reporter assays. (A). Chemical structures of AZ12601011 (previously undisclosed) and AZ12799734 (Goldberg et al., 2009). (B) TGFβ-inducible SMAD3/4 dependent CAGA$_{12}$ promoter-luciferase reporter bioassay carried out both in the absence (-) and presence (+) of exogenous addition of TGFβ1 (1ng/mL) for 8 hours. Stably transfected NIH 3T3 CAGA$_{12}$ cells were pre-treated with a titration of SB-431542, SB-525334, AZ12601011, AZ12799734 or LY2157299 for 15 minutes prior to induction of luciferase activity by exogenous TGFβ addition. The mean (± S.D.) activity (as a % of the control cells + TGFβ) is shown from a representative experiment. (C) Representative dose response curves of TGFBR1 inhibitors generated from CAGA$_{12}$ bioassays as shown in (B). Data is presented as a percentage of luciferase activity of untreated control cells + TGFβ (100%). (D) Mean ± s.d. IC$_{50}$ determined by median effect plots using CalcuSyn curve fit software and IC$_{50}$ and 95% confidence intervals determined by non-linear regression analysis using Graphpad Prism 7 software are shown. The IC$_{50}$s were generated from replicate independent dose response curves AZ12601011 (n=4), AZ12799734 (n=3), SB-525334 (n=4), SB-431542 (n=5), LY2157299 (n=4).

Figure 2. Inhibition of TGFβ-induced phosphorylation of SMAD2 by AZ12601011. (A) Representative SDS-PAGE and western blot analysis for phosphorylated SMAD2 and total SMAD2 of RIPA lysates from two independent experiments where cell lines pre-treated with a titration of AZ12601011 for 20 minutes followed by exogenous addition of TGFβ (5ng/mL) for 1 hour. (B-D) LI-COR odyssey infrared imaging quantification of phospho-SMAD2 (ser465/467) normalised to pan-SMAD2 levels in HaCaT cells pre-treated with a titration of AZ12601011 (range 10μM – 0.01μM) prior to TGFβ addition for 1 hour (n=3). Representative scanned blots (B) and combined raw intensity signals from infrared imaging of pan-SMAD2 and phospho-SMAD2 western blots - lane 2 (untreated + TGFβ) (C). (D) Bar chart depicting the mean ± s.e.m (n=3) ratio of phospho-SMAD2 normalised signal intensity relative to the untreated control (lane1) from replicate assays.

26

Figure 3. Assessment of TGFBR1 inhibitors in *in vitro* culture systems. (A) NIH3T3 CAGA$_{12}$-luciferase cells were left untreated or pre-treated for 15 minutes with 20nM AZ12601011 and 60nM AZ12799734 that had undergone the indicated number of freeze thaw cycles. Following pre-treatment, the reporter cells were stimulated with 1ng/mL TGFβ for 8 hours, lysed and the relative luciferase units (RLU) measured. Results are presented as the mean RLU (± S.D.) normalised to protein content of the lysate of three replicate wells. (B) Cell culture media (DMEM + 10% FBS) was spiked with 10μM inhibitors and incubated at 37ºC for the times indicated. On Day 9, HaCaT cells were seeded at overnight at 5x10^4 in 24-well plates. Media was removed from the wells and replaced with inhibitor spiked media for 15 minutes pre-treatment prior to addition of TGF-β at 5ng/mL for 2 hours. Cell lysates were analysed by SDS-PAGE and western blot for phosphorylated SMAD2 and β-Actin as a loading control (n=1). (C) 1x10^6 VU-SCC-040 cells were seeded overnight into 10cm dishes and treated with solvent control (DMSO), SB-431542, Galunisertib, AZA12601011 or AZ12799734 at 10μM final concentration. Treated cells were incubated for the times shown and then challenged with exogenous TGFβ1 (5ng/mL) for 2 hours. Cell lysates were analysed by SDS-PAGE and western blot for phosphorylated SMAD2 and β-Actin as a loading control. Representative western blots from replicate biological experiments (n=2) showing similar results are shown.

Figure 4. Selectivity of AZ12601011 and AZ12799734 against TGFβ superfamily type 1 receptors. (A, B) 4.5 x 10^4 NIH3T3 cells were seeded in 24-well plates and incubated overnight. Cells were transfected with 100ng CAGA$_{12}$-luciferase reporter and 150ng plasmids expressing constitutively active (*) type 1 receptors ALK4, TGFBR1 or ALK7. After 24 hours the relative luciferase activity was measured in cell lysates. RLUs were normalised to protein content and expressed as the mean RLU (± S.D.) from a minimum of 3 replicate wells. (B) Cells were transfected as described in (A) and treated with a titration of either AZ12601011 or AZ12799734 as indicated. Results are shown as the mean percent RLU (± S.D.) relative to control samples. (C) NIH3T3 cells were co-transfected in singlicate

with 500ng SMAD1 or SMAD2 expression plasmids and 500ng plasmids expressing constitutively active (*) receptors. Cells were either left untreated or treated with 10μM AZ12601011 or AZ12799734 for 24 hours prior to lysis and analysis of lysates by SDS-PAGE and western blotting for the proteins indicated.

Figure 5. Selectivity of AZ12601011 and AZ12799734 in cell based assays. (A) C2C12-BRE-LUC cells were pre-treated with a titration of AZ12601011 and AZ12799734 for 20 minutes prior to addition of 5ng/mL recombinant BMP ligand. Luciferase activity was measured using the Luciferase assay system (Promega). Results presented are the mean fold activation of the luciferase reporter in response to ligand relative to activity in untreated cells. (B, C) Serum starved (0.1% FBS) NIH3T3 cells were pre-treated in singlicate with a titration of AZ12601011 (as indicated) for 20 minutes prior to stimulation for 5 minutes with EGF (30ng/mL) (B) or osmotic shock treatment for 20 minutes with NaCl (0.7M) (C). U0126 treatment at 25μM was included as a positive control for inhibition of EGF signalling via the MAPK pathway (B). Cells were then washed in ice cold PBS and lysed in RIPA. Protein lysates were quantified and equal amounts of protein analysed by SDS-PAGE and western blots for the proteins indicated are shown.

Figure 6: Blockade of TGFβ-induced migration. HaCaT cells were seeded at 15,000 cells/well in ImageLock plates (Essen Biosciences) and incubated overnight. Cells were washed twice in PBS and serum starved for 24 hours in DMEM supplemented with 0.2% FBS. Uniform wounds were generated using a Woundmaker, the cells washed twice in PBS, and then pre-treated with titrations of SB-431542, AZ12601011 or AZ12799734 in DMEM/0.2% FBS followed by BSA/HCL carrier control or TGFβ (5ng/mL). Closure of the wound was monitored by IncuCyte Zoom imaging over 4 days. Data presented is the mean ± S.E.M of a minimum of three replicate wells taken from a representative experiment.

Figure 7: *In vivo* **profile of TGFBR1 inhibitors.** (A) Total and free PK levels of AZ12601011 and AZ12799734 in the nude mouse following 50mg/kg *per oral* dose, with time over *in vitro* IC_{50} (0.01582μM and 0.01885μM respectively). (B) Growth of 4T1 cells (shown as a percentage of vehicle treated control cells) treated with AZ12601011. Growth was determined after 4 days treatment using the IncucyteZoom real time imaging system. (C) PD modulation of pSMAD2 levels following treatment for with AZ12601011 (50mg/kg BID) in the mouse 4T1 syngeneic cell line grown via mammary orthotopic implant. pSMAD2 levels were measured in tumour cell lysates by ELISA 1hour after drug administration. (D) Mouse 4T1 syngeneic orthotopic tumour growth over 25 days in vehicle control (n=13) and AZ12601011 (50mg/kg BID) (n=10) treated mice. Mice were treated by oral gavage twice daily from day 1 following implant. Tumour volumes in individual mice are shown. (E) Mean ± SEM tumour volumes of all mice in the vehicle control and AZ12601011 treated groups until day of first sacrifice (Day 18). Statistical analysis was carried out by pairwise comparison using the compareGrowthCurves function in statmod (R project). The adjusted p value is shown. (F) Kaplan-meier plots showing statistically significant differences in event-free (left) [Log Rank (Mantel-Cox) χ2(1) = 9.191, p < .002] and tumour <0.5cm^3 (right) [Log Rank (Mantel-Cox) χ2(1) = 17.448, p = 0.00003] survival. (Control group n=13; Treated group n=10). (G) Scatterplot showing relative lung metastasis scores in the 4T1 syngeneic orthotopic tumour mice (described in D to F) following vehicle control (n=12) or AZ12601011 treatment (n=10). The scatterplot points represent individual mice, and bars represent the median and the interquartile ranges. Analysis was carried out using Mann-Whitney U test. AZ12601011 treated group (median = 1); vehicle control group (median = 4), U = 26, z = -2.267, p = .025, using an exact sampling distribution for U.
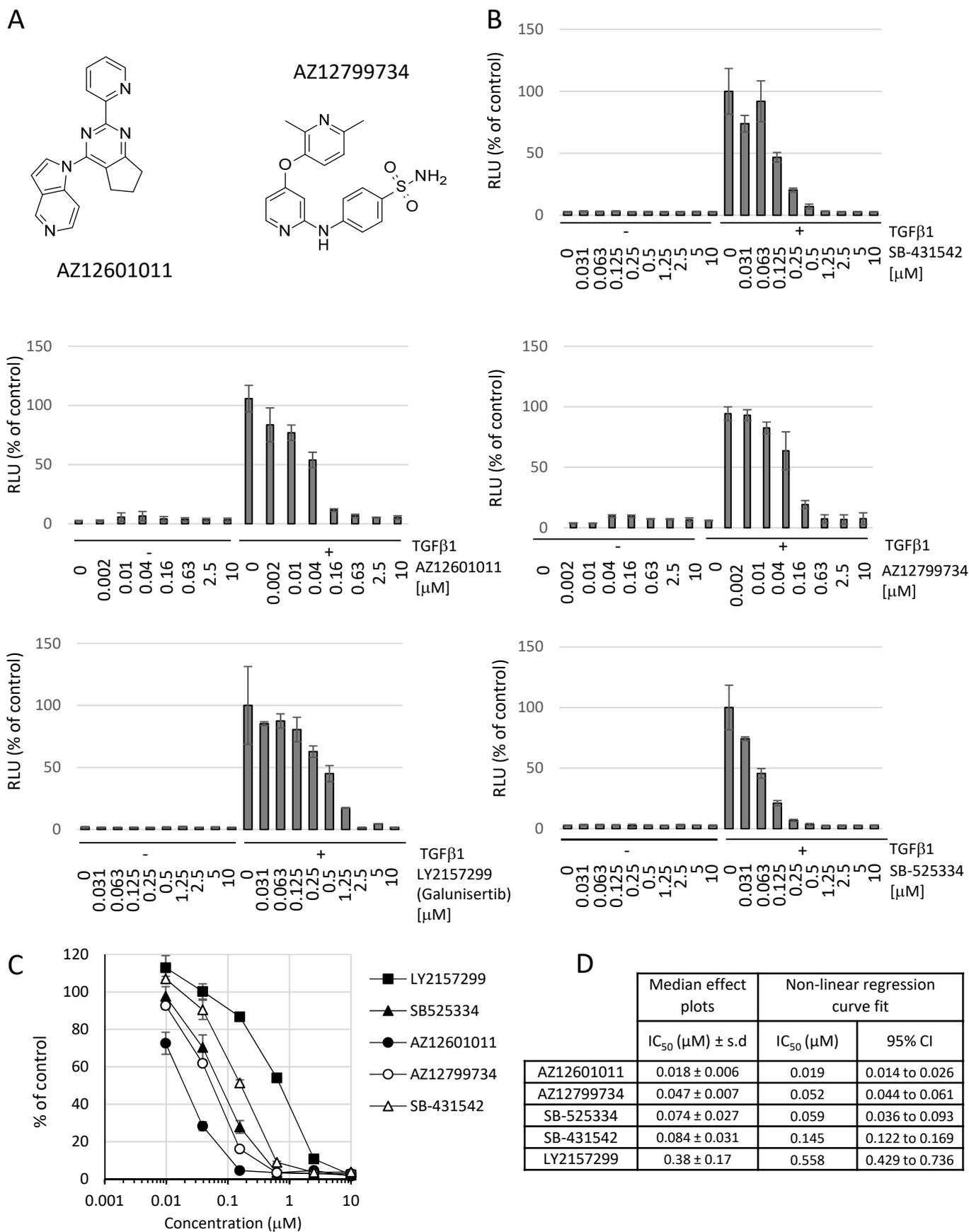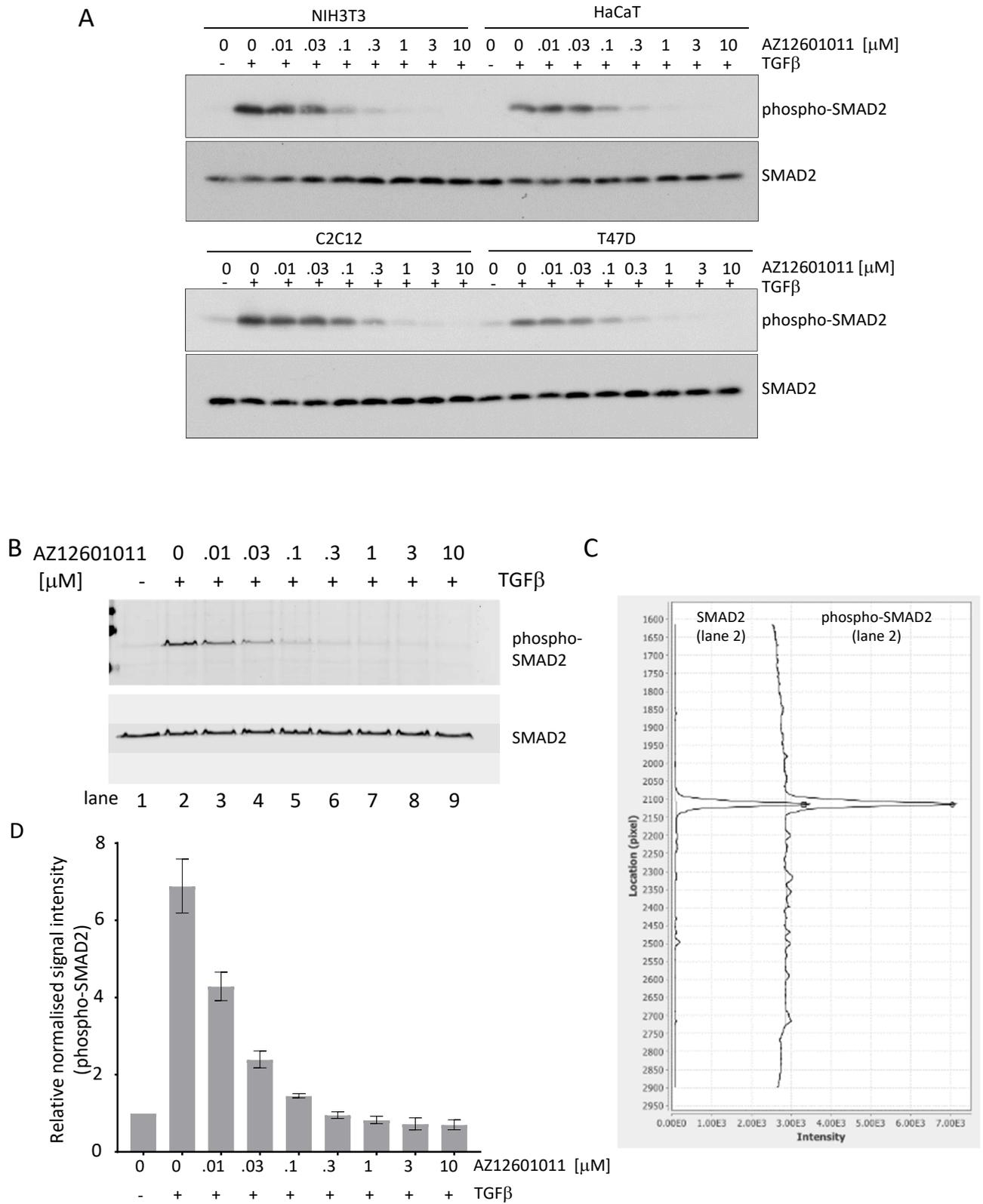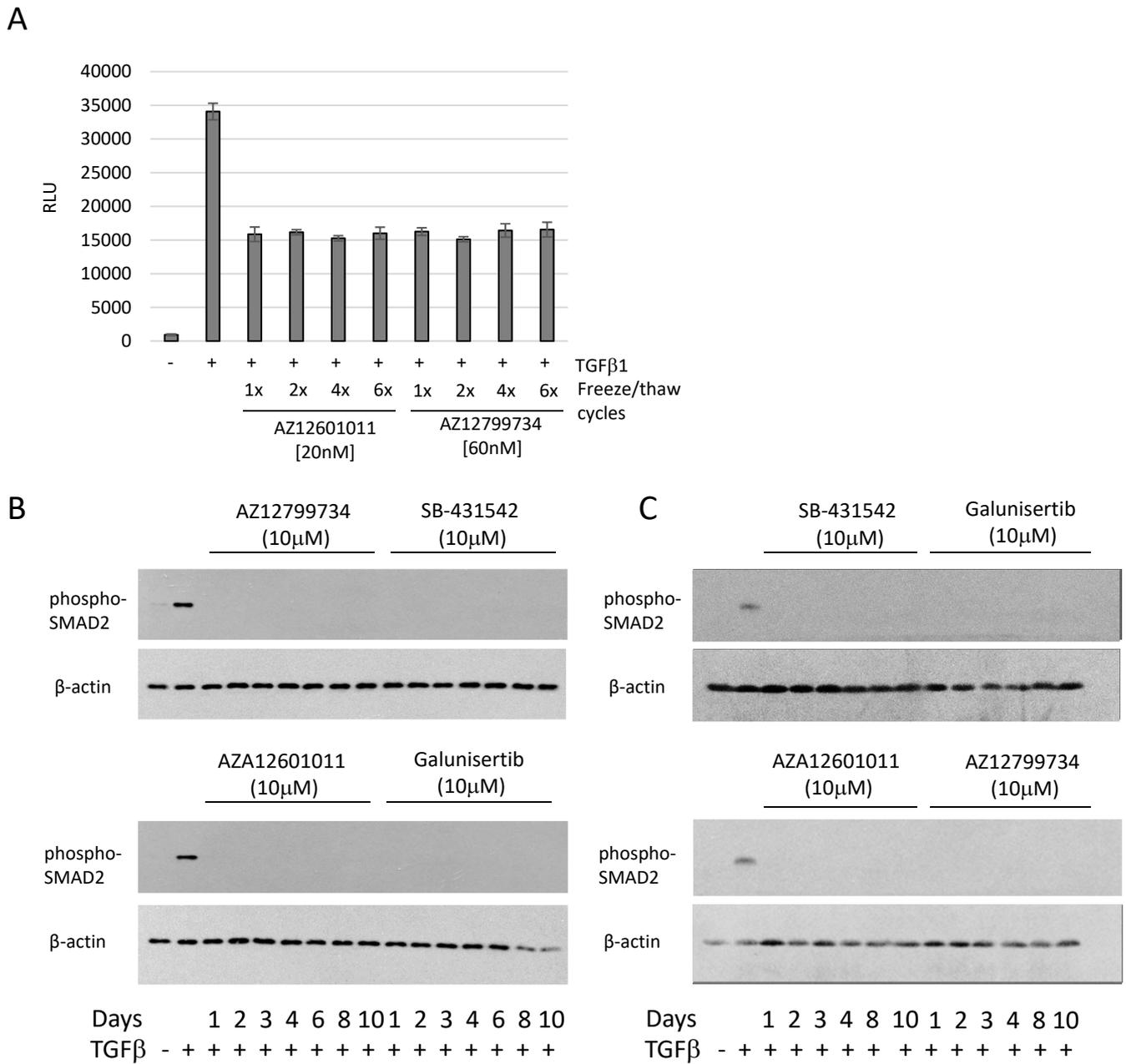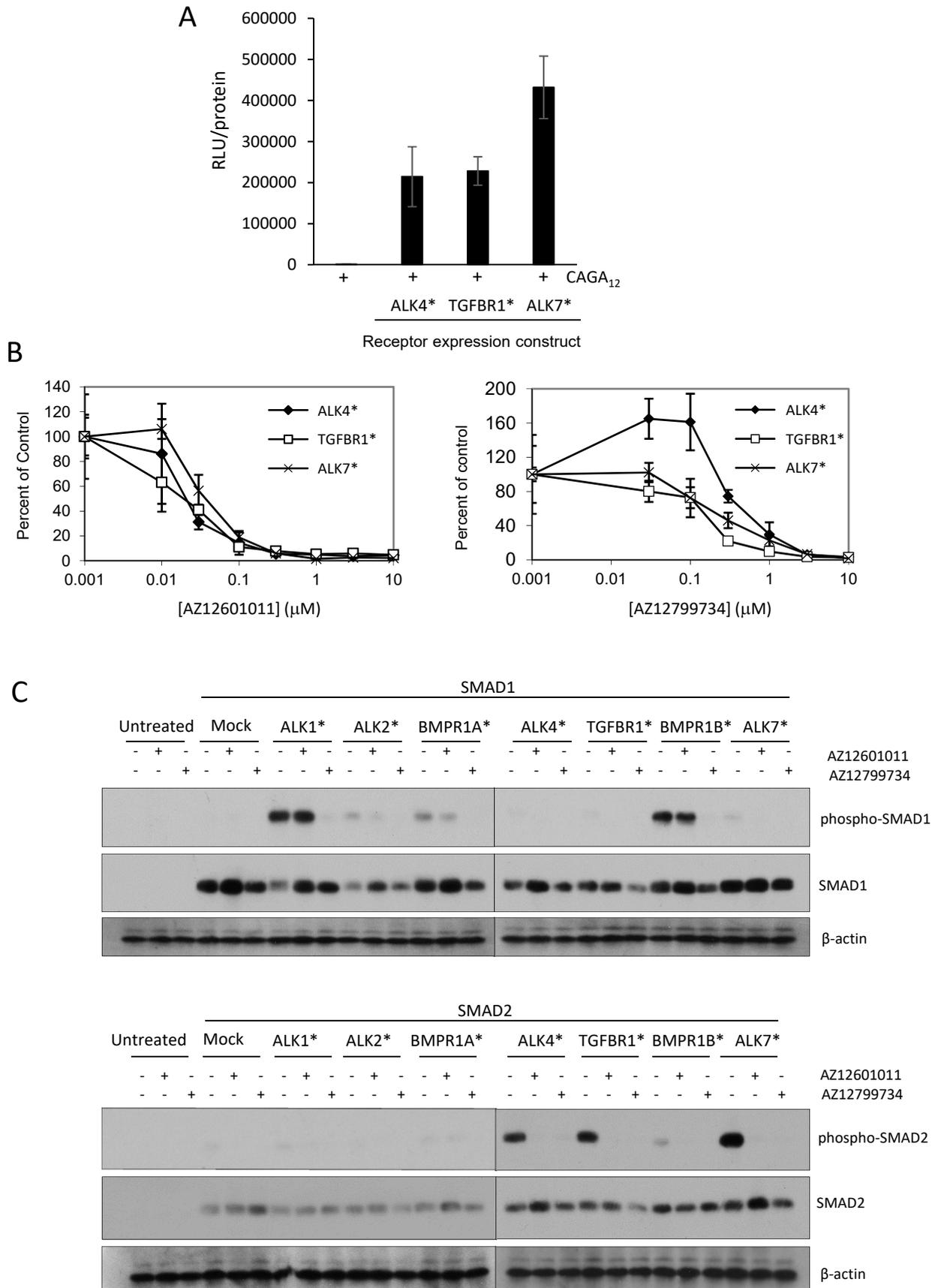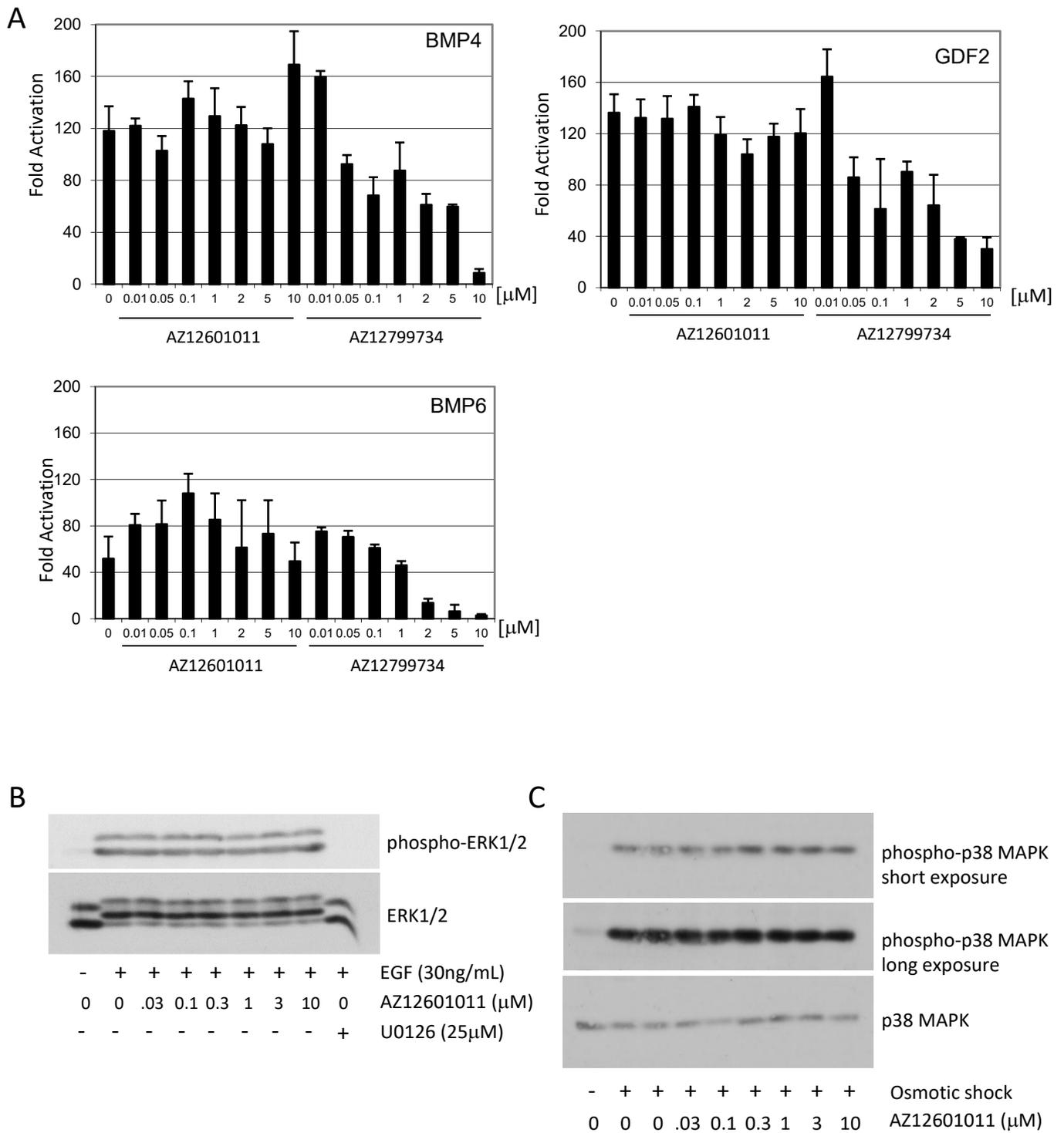
Figure 1

Figure 2

Figure 3

Figure 4

Figure 5

Figure 6

Figure 7